Verification of finite element simulations of wave-plasma interactions in space electric propulsion devices

Mario Merino[(1)], Hugo Bergerioux[(1)], Pedro Jiménez[(1)], Marco Inchingolo[(1)], Jaume Navarro-Cavallé[(1)]
mario.merino@uc3m.es
[(1)]Universidad Carlos III de Madrid, Department of Aerospace Engineering, 28911 Leganés (Madrid), Spain

***Abstract*—The operation of various types of space plasma thrusters relies on heating the plasma with electromagnetic waves, typically in the MHz or GHz range. This is the case of electrodeless plasma thrusters. To understand and characterize the propagation and absorption of electromagnetic power by the magnetoplasma, a commonly-used approach is to model the plasma as a linear, anisotropic, gyrotropic, dissipative medium based on the cold-plasma assumption. Simulation codes ranging from finite differences (e.g. Yee scheme) to finite elements (e.g. Nédélec edge elements) are used to find the response of the wavefields to a given geometry, plasma density, and applied magnetic field profiles. This presentation reviews recent efforts at Universidad Carlos III de Madrid to simulate electrodeless plasma thrusters with finite element schemes, and the occurrence of spurious wave solutions whenever the propagation regime includes so-called resonant cones. To characterize the spurious solutions, we set up a verification simulation case based on the Fresnel problem for a planar wave propagating in vacuum and into a plasma, and compare against the analytical solution. We find perfect agreement with our finite element solution, except for parametric regimes where the plasma has resonant cones. Analysis of the analytical and numerical dispersion relations helps identify the sources of error, and potential countermeasures are proposed.**

I. Introduction

Space plasma propulsion powers more than half of existing satellites in orbit [1]. It excels over chemical propulsion in terms of specific impulse, I_{sp}, which defines the exhaust velocity and the propellant consumption in any given mission. The lower expense of propellant makes plasma propulsion advantageous in terms of economics and mission lifetime.

Electrodeless Plasma Thrusters (EPTs) rely on power deposition from electromagnetic waves to heat the plasma [2]. In particular, waveguide-based Electron-Cyclotron Resonance Thrusters (ECRTs) use resonant microwave absorption [3]. At Universidad Carlos III de Madrid, the hybrid PIC-fluid code HYPHEN-EPT has been developed to simulate plasma discharge, incorporating a two-dimensional, full-wave model [4], [5]. The general scheme of the HYPHEN-EPT code can be seen in figure 1, and the typical simulation domain (including a segment of waveguide) is shown in figure 2. HYPHEN-EPT works by alternating the solution of the slow plasma transport fields and the fast electromagnetic fields. Both aspects of the simulation are coupled, as the wave block requires the plasma density and collisionality maps, and the transport block relies on the power deposition profile. The wave block solves Maxwell's equations in the frequency domain using a finite element discretization (using Nédélec elements), and describes the linearized plasma response to

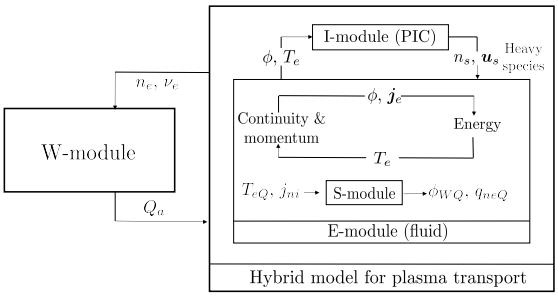

Fig. 1: Code structure of the HYPHEN-EPT code. The slow transport block contains modules for the heavy species (Particle-in-Cell, I-module), the light electrons (fluid, E-module), and plasma sheaths (S-module). The fast EM fields block (W-module) is solved every few time steps of the transport module to update the wave propagation and absorption profiles; the wave absorption map, Q_a, defines the source terms in the transport simulation.

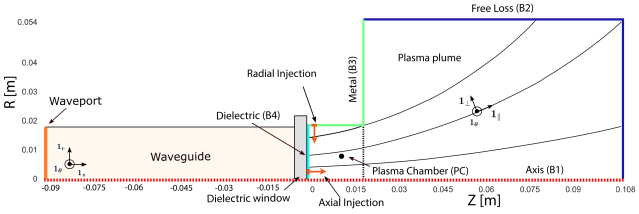

Fig. 2: Typical simulation domain for the ECRT studies. A wave is launched from the left through a waveguide port. It traverses a dielectric window and access the ionization chamber of the thruster, where it interacts with the plasma. From [7].

electromagnetic fields through the cold-plasma approximation [6]. This dielectric tensor approximation in this limit takes the following form in a magnetic-field-aligned vector basis:

$$\overline{\overline{\varepsilon}} = \begin{bmatrix} S & -iD & 0 \\ iD & D & 0 \\ S & 0 & P \end{bmatrix} \tag{1}$$

where $S = (R+L)/2$ $D = (D-L)/2$ and P are the usual parameters as defined in [6].

The ECRT (and many other plasma devices) is character-

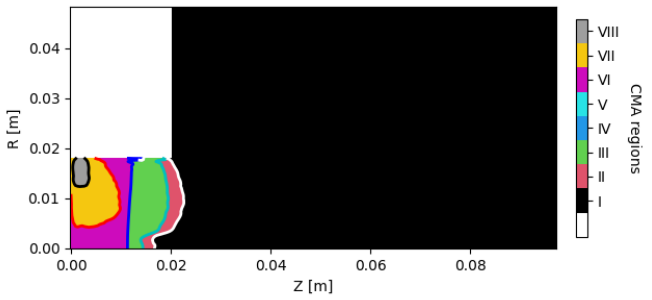

Fig. 3: Parametric regions of wave propagation in the simulated ECRT discharge chamber and external region, according to the nomenclature of Stix [6].

ized by a succession of transitions among wave propagation regimes in a small volume, dependent upon two key parameters: the applied magnetic field strength and the plasma density. The interaction of the wave with the free electrons in the plasma gives rise to a strongly anisotropic, gyrotropic, and dissipative response. An example of the parametric regimes found in the small ECRT domain can be seen in figure 3, based on the nomenclature of Stix [6]. Crucially, regions III, VII and VIII feature 'resonant cones', i.e., propagation of waves only within a cone around the magnetic field direction, and a resonance at the cone edge ($k \to \infty$ in the collisionless, i.e. non-dissipative limit).

Recent hybrid PIC/fluid + wave simulations of the EP2 waveguide ECRT prototype [7] provided insights into the energy deposition and plasma loss mechanisms, but also revealed intricate short-wavelength interference patterns, which were found to be related to resonance cones in the parametric wave regime where the device operates. However, these small wave structures, illustrated in figure 4, were found to be close to the mesh size and did not show good convergence with it, raising the question of their numerical accuracy.

Indeed, in the limit of planar waves with a collisionless dielectric tensor $\overline{\overline{\varepsilon}}$ of the form in equation (1) and wavenumber vector $\boldsymbol{k}$, the resonance cones occur at an angle $\theta = \arctan(-P/S)$ from the applied magnetic field vector. If we split the wave complex electric field magnitude $\boldsymbol{E}$ into its electrostatic (longitudinal, irrotational) and electromagnetic (transverse, solenoidal) components, $\boldsymbol{E} = \boldsymbol{E}_k + \boldsymbol{E}_{em}$, with $\boldsymbol{E}_k = E_k \mathbf{1}_k$, the wave equation reads

$$\overline{\overline{\varepsilon}} \cdot (\mathbf{1}_k E_k + \boldsymbol{E}_{em}) - k^2 \boldsymbol{E}_{em} = \mathbf{0}. \tag{2}$$

As we approach the resonance cones (but still within the propagating angles), $k \to \infty$ and the wave is essentially electrostatic with $\boldsymbol{E}_m \simeq \mathbf{0}$ but $\neq \mathbf{0}$. Then, the wave equation (2) becomes ill-posed numerically, as $k^2 \gg |\overline{\overline{\varepsilon}}|$. The situation ameliorates partially with the introduction of artificial damping (e.g. extra plasma collisionality), which limits the growth of the real part of k.

While the presence of these small structures was found to have a relatively small impact on power deposition, resolving this uncertainty is key to refining simulation accuracy and deepening our understanding of wave-plasma interactions in such thrusters.

To address the question of the non-physicality of these

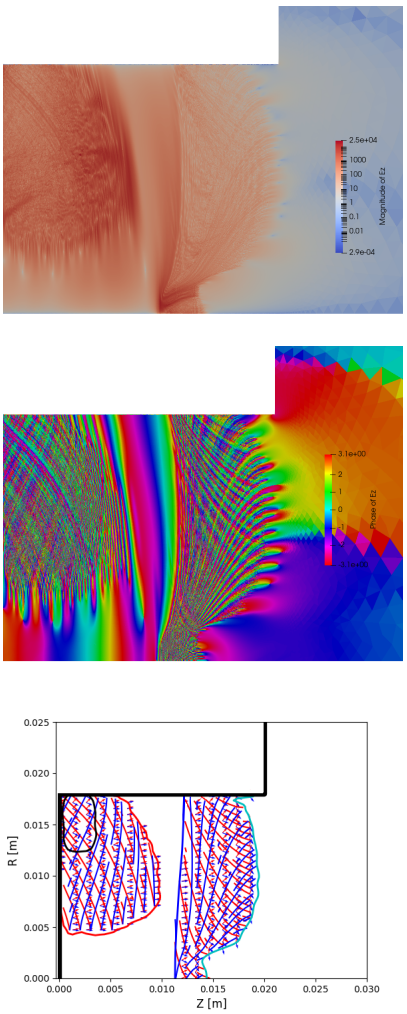

Fig. 4: First two plots: Magnitude and phase of the E_z wavefield component, illustrating the intricate fine-structure waves found in regions with resonant cones that are believed to be spurious solutions. Last plot: diagram of the local direction of the resonant cones, showing a pattern match with the fine structures.

wave structures, we resort to a clean verification problem with analytical solution: a generalized Fresnel problem of a planar wave traveling from a semi-infinite vacuum to a semi-infinite, uniform magnetoplasma. We first present the analytical derivation of the relevant Fresnel relations to describe wave reflection and transmission at the interface between these two media, as a function of the wave polarization, incidence angle, plasma parameters, and magnetic field direction. A new version of the W-module has been developed during this study, implemented in Julia/Gridap [8], [9], which provides better compute times and higher flexibility than the previous version, based on Python/Fenicsx. Our preliminary results, presented in figure 5, verify the new W-module code through direct comparison with the analytically derived Fresnel relations. The plots illustrate the accuracy of the numerical model accuracy in handling wave interactions at vacuum-magnetoplasma interfaces for a particular set of parameters, and this is seen to hold equally well for all parametric regimes without resonance cones.

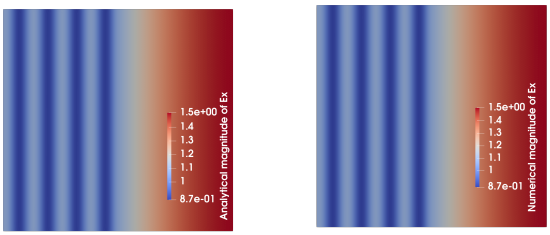

Fig. 5: Comparison of the analytical (left) and numerical (right) solutions to the Fresnel problem between vacuum and magnetoplasma, for the magnitude of the E_x wavefield component, in a parametric region without resonance cones (region I in Stix's nomenclature [6]).

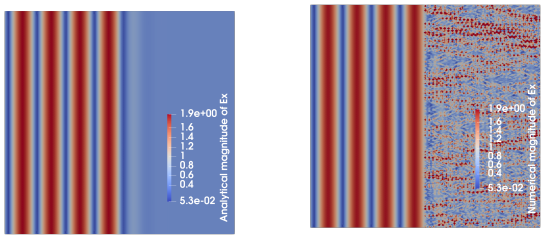

Fig. 6: Comparison of the analytical (left) and numerical (right) solutions to the Fresnel problem between vacuum and magnetoplasma, for the magnitude of the E_x wavefield component. Plasma parameters correspond respectively to Regions I and VIII according to the nomenclature of Stix [6].

Nevertheless, when the plasma on the right side of the Fresnel problem is set to a parametric regime with the presence of resonant cones, artificial fine structures appear in the numerical solution, which are absent in the analytical solution, as observed in figure 6. This allows us to conclude that regular techniques are not suitable for wave-plasma simulations whenever this parametric regimes arise anywhere in the simulation domain.

In addition to the ill-posedness of the problem described above, a characterization of the analytical and numerical dispersion relations in $k-\theta$ space (not shown) further reveals major differences at large k values, which are believed to be also related to the poor numerical solution in the presence of resonant cones.

Potential solutions to the issue found in this study call for the regularization of the wave equation. Progress in related settings was made by Otin [10], who introduced a regularization term based on the divergence equation for $\boldsymbol{E}$. This and similar approaches may enable the correct simulation of wavefields in electric propulsion devices and other technological plasmas.

Acknowledgments: This work has received funding from the European Research Council (ERC) under the European Union's Horizon 2020 research and innovation programme (Starting Grant ZARATHUSTRA, grant agreement No 950466).

REFERENCES

[1] D. Lev, R. M. Myers, K. M. Lemmer, J. Kolbeck, H. Koizumi, and K. Polzin, "The technological and commercial expansion of electric propulsion," *Acta Astronautica*, vol. 159, pp. 213–227, 2019.

[2] S. Bathgate, M. Bilek, and D. Mckenzie, "Electrodeless plasma thrusters for spacecraft: a review," *Plasma Science and Technology*, vol. 19, no. 8, p. 083001, 2017.

[3] M. R. Inchingolo, M. Merino, M. Wijnen, and J. Navarro-Cavallé, "Thrust measurements of a waveguide electron cyclotron resonance thruster," *Journal of Applied Physics*, vol. 135, 3 2024.

[4] A. Sánchez-Villar, J. Zhou, M. Merino, and E. Ahedo, "Coupled plasma transport and electromagnetic wave simulation of an ECR thruster," *Plasma Sources Science and Technology*, vol. 30, no. 4, p. 045005, 2021.

[5] P. Jiménez, M. Merino, and E. Ahedo, "Wave propagation and absorption in a helicon plasma thruster source and its plume," *Plasma Sources Science and Technology*, vol. 31, no. 4, p. 045009, 2022.

[6] T. H. Stix, *Waves in plasmas*. Springer Science & Business Media, 1992.

[7] M. R. Inchingolo, P. Jiménez, J. Zhou, M. Merino, and J. Navarro-Cavallé, "Simulation of the discharge and microwave-plasma coupling in a waveguide ECR thruster," in 38th *International Electric Propulsion Conference*, no. IEPC-2024-592, (Toulouse, France, June 23-28), Electric Rocket Propulsion Society, 2024.

[8] S. Badia and F. Verdugo, "Gridap: An extensible finite element toolbox in julia," *Journal of Open Source Software*, vol. 5, no. 52, p. 2520, 2020.

[9] F. Verdugo and S. Badia, "The software design of gridap: A finite element package based on the julia JIT compiler," *Computer Physics Communications*, vol. 276, p. 108341, July 2022.

[10] R. Otin, "Regularized Maxwell Equations and Nodal Finite Elements for Electromagnetic Field Computations," *Electromagnetics*, vol. 30, pp. 190–204, Mar. 2010.